Smoothelin-B deficiency results in reduced arterial contractility, hypertension, and cardiac hypertrophy in mice

Smoothelin-B Deficiency Results in Reduced Arterial Contractility, Hypertension, and Cardiac Hypertrophy in Mice

Sander S. Rensen, PhD; Petra M. Niessen, PhD; Jan M. van Deursen, PhD; Ben J. Janssen, PhD; Edwin Heijman, MS; Evelien Hermeling, MS; Merlijn Meens, MS; Natascha Lie, MD; Marion J. Gijbels, PhD; Gustav J. Strijkers, PhD; Pieter A. Doevendans, MD, PhD; Marten H. Hofker, PhD; Jo G.R. De Mey, PhD; Guillaume J. van Eys, PhD

Background—Smoothelins are actin-binding proteins that are abundantly expressed in healthy visceral (smoothelin-A) and vascular (smoothelin-B) smooth muscle. Their expression is strongly associated with the contractile phenotype of smooth muscle cells. Analysis of mice lacking both smoothelins (*Smtn-A/B*$^{-/-}$ mice) previously revealed a critical role for smoothelin-A in intestinal smooth muscle contraction. Here, we report on the generation and cardiovascular phenotype of mice lacking only smoothelin-B (*Smtn-B*$^{-/-}$).

Methods and Results—Myograph studies revealed that the contractile capacity of the saphenous and femoral arteries was strongly reduced in *Smtn-B*$^{-/-}$ mice, regardless of the contractile agonist used to trigger contraction. Arteries from *Smtn-A/B*$^{-/-}$ compound mutant mice exhibited a similar contractile deficit. *Smtn-B*$^{-/-}$ arteries had a normal architecture and expressed normal levels of other smooth muscle cell–specific genes, including smooth muscle myosin heavy chain, α-smooth muscle actin, and smooth muscle-calponin. Decreased contractility of *Smtn-B*$^{-/-}$ arteries was paradoxically accompanied by increased mean arterial pressure (20 mm Hg) and concomitant cardiac hypertrophy despite normal parasympathetic and sympathetic tone in *Smtn-B*$^{-/-}$ mice. Magnetic resonance imaging experiments revealed that cardiac function was not changed, whereas distension of the proximal aorta during the cardiac cycle was increased in *Smtn-B*$^{-/-}$ mice. However, isobaric pulse wave velocity and pulse pressure measurements indicated normal aortic distensibility.

Conclusions—Collectively, our results identify smoothelins as key determinants of arterial smooth muscle contractility and cardiovascular performance. Studies on mutations in the *Smtn* gene or alterations in smoothelin levels in connection to hypertension in humans are warranted. **(*Circulation*. 2008;118:828-836.)**

Key Words: hypertension ■ hypertrophy ■ muscle contraction ■ muscle, smooth ■ vascular resistance

Hypertension is a common condition in Western countries, affecting ≈27% of the population worldwide. It is a major risk factor for the development of life-threatening conditions such as coronary heart disease and stroke. However, the cause of increased blood pressure is unknown in most patients.[1] Smooth muscle contractility is one of the primary determinants of vascular resistance, thereby contributing significantly to the maintenance of a physiological blood pressure. Accordingly, molecular defects in the regulation or mechanics of arterial smooth muscle contraction generally cause profound cardiovascular phenotypes. For example, α-smooth muscle actin (α-SMA) knockout mice display impaired vascular contractility and reduced blood flow.[2] Likewise, smooth muscle myosin heavy chain (SM-MHC)-B knockouts show a significant decrease in maximal shortening velocity of vascular smooth muscle,[3] and SM-calponin–deficient mice have impaired mean arterial pressure (MAP) regulation.[4]

Clinical Perspective p 836

Despite the importance of smooth muscle cell (SMC) contraction for the cardiovascular system, the contractile process itself is still incompletely understood. In particular, the functions of regulatory proteins that are connected to the actin-myosin filaments in vascular SMCs remain poorly defined.[5] Candidate thin filament regulatory proteins that have not been studied in this respect are the smoothelins, which are α-SMA–binding

Received October 4, 2007; accepted June 20, 2008.

From the Departments of Genetics and Cell Biology (S.S.R., P.M.N., N.L., M.J.G., M.H.H., G.J.v.E.), Pharmacology and Toxicology (B.J.J., M.M., J.G.R.D.M.), Biophysics (E. Hermeling, G.J.S.), and Cardiology (P.A.D.), Cardiovascular Research Institute Maastricht, Maastricht University, Maastricht, the Netherlands; Department of Pediatrics and Adolescent Medicine, Mayo Clinic, Rochester, Minn (J.M.v.D.); and Biomedical NMR, Department of Biomedical Engineering, Eindhoven University of Technology, Eindhoven, the Netherlands (E. Heijman, G.J.S.).

Drs Rensen, Niessen, and van Deursen contributed equally to this work.

The online-only Data Supplement can be found with this article at http://circ.ahajournals.org/cgi/content/full/CIRCULATIONAHA.107.743690/DC1.

Correspondence to G. van Eys, PhD, Department of Genetics and Cell Biology, Maastricht University, PO Box 616, 6200 MD Maastricht, the Netherlands. E-mail g.vaneys@gen.unimaas.nl

Circulation **is available at http://circ.ahajournals.org** **DOI: 10.1161/CIRCULATIONAHA.107.743690**

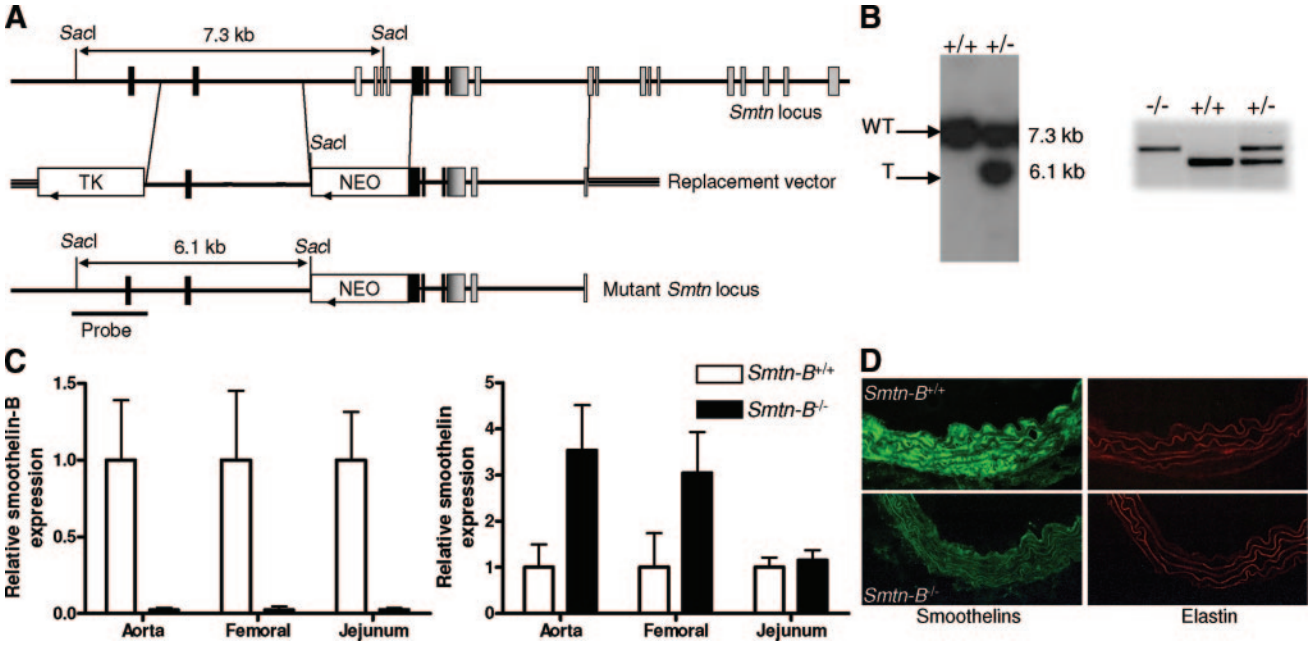

Figure 1. Targeting of the *Smtn* gene for the generation of mice lacking smoothelin-B. A, Schematic of the targeting strategy. Top, Structure of the *Smtn* gene. Black boxes indicate smoothelin-B exons; light gray boxes, exons common to smoothelin-A and -B; and white boxes, targeted exons. Middle, *Smtn-B*$^{-/-}$ targeting vector containing neomycin resistance (NEO) and herpes simplex virus thymidine kinase (TK) genes, both transcribed in the reverse direction to that of the *Smtn* gene, as indicated by arrows. Bottom, Structure of the targeted *Smtn* allele and location of the probe used in Southern blot analyses after *Sac*I digestion. The distance between the *Sac*I sites in the wild-type (top) and mutant (bottom) locus is shown. B, Left, Southern blot analyses of genomic DNA from wild-type and targeted ES cells after *Sac*I digestion with the probe indicated above (in A). The wild-type *Sac*I fragment (WT) is 7.3 kb; the mutant *Sac*I fragment (T) is 6.1 kb. Right, PCR analyses of genomic DNA from *Smtn-B*$^{+/+}$, *Smtn-B*$^{+/-}$ and *Smtn-B*$^{-/-}$ mice. The +/+ and −/− PCR fragments are 191 and 240 bp, respectively. C, Q-PCR analysis showing absent smoothelin-B expression in aorta, femoral artery, and jejunum of *Smtn-B*$^{-/-}$ mice (left; n=6 for each genotype). Q-PCR experiments using primers and probes directed against the part that both smoothelins have in common revealed upregulated expression of either smoothelin-A or an interrupted smoothelin-B transcript in blood vessels but not in jejunum (right; n=6 for each genotype). D, Cross sections of aortas of *Smtn-B*$^{+/+}$ and *Smtn-B*$^{-/-}$ mice were stained for smoothelin-A and -B (green; ×400 magnification). The cells between the autofluorescent elastic laminae do not stain, showing that smoothelins are not present in vascular SMCs of *Smtn-B*$^{-/-}$ mice. Right, Autofluorescence of the elastic laminae is shown in red.

proteins specifically and abundantly expressed in contractile SMCs.[6–9] They are encoded by a single-copy gene that generates 2 major isoforms, both containing a troponin T–like domain.[10] The smaller smoothelin-A isoform is expressed most prominently in visceral SMCs. In contrast, the 110-kDa smoothelin-B, which is encoded by the smoothelin-A exons plus 10 upstream exons, is found only in vascular SMCs.[11] Smoothelin-B expression is particularly high in muscular arteries, whereas expression in elastic arteries is modest.[7]

In recent years, smoothelin-B has been increasingly recognized as an excellent marker of the so-called contractile phenotype of vascular SMCs. Indeed, loss of smoothelin-B expression reliably indicates the disappearance of the contractile SMC phenotype in various vascular disorders ranging from aortic aneurysms to atherosclerosis and restenosis.[9,12–16]

Functional studies on smoothelins have been hampered by the rapid downregulation of their expression in vitro and their relative insolubility at physiological ionic concentrations.[6] Therefore, despite its relevance for the characterization of the contractile SMC phenotype, the function of smoothelin-B in vascular SMCs has remained elusive. Recently, however, we showed that smoothelin-A plays a crucial role in intestinal SMC contraction in mice.[17] *Smtn-A/B*$^{-/-}$ mice, which lack both smoothelin isoforms, develop fatal intestinal problems as a result of drastically decreased intestinal SMC contractility. The severe impact of smoothelin-A deficiency on visceral smooth muscle contraction suggests that smoothelin-B might play an equally important role in vascular smooth muscle. To test this hypothesis, we generated mice lacking only smoothelin-B (*Smtn-B*$^{-/-}$) and investigated their cardiovascular physiology. We report that smoothelin-B–deficient mice show reduced arterial contractility, which is paradoxically accompanied by elevated MAP because of increased peripheral vascular resistance.

Methods

Generation of *Smtn-B*$^{-/-}$ Mice

To generate *Smtn-B*$^{-/-}$ mice, we targeted exons 3 through 7 with a neomycin gene under the control of the thymidine kinase promoter in reverse orientation (Figure 1A). Targeting of embryonic stem cells and germline transmission of the targeted alleles were detected by Southern blotting and polymerase chain reaction (PCR) analysis (Figure 1B; see the online-only Data Supplement for a list of primers). Mice were further backcrossed at least 5 times on C57Bl/6 background before initiation of experiments. Because the mice had a mixed background, we used littermates for experimentation. All animal experiments were approved by the Maastricht University animal ethics committee.

Quantitative Reverse-Transcriptase PCR

Total RNA was extracted from jejunum, hearts, or pooled aortas and femoral arteries from *Smtn-B*$^{+/+}$ and *Smtn-B*$^{-/-}$ mice with Trireagent (Sigma-Aldrich, Zwijndrecht, the Netherlands). Reverse

transcription was performed with the iScript cDNA synthesis kit (Biorad, Veenendaal, the Netherlands) and 0.5 or 1 μg RNA. Expression of several transcripts was investigated by quantitative PCR (Q-PCR) with the ABIPrism7700 System (Perkin Elmer, Norwalk, Conn). Applied primers and probes are listed in the supplemental table. The cyclophilin A transcript was used to normalize the amount and quality of the extracted RNA. *Smtn-B*$^{+/+}$ expression levels were set at 1.

Histology and Immunohistochemistry

Organs from mice 2 months and 1 year of age were fixed in 3.7% formaldehyde in PBS, embedded in paraffin, sectioned, and stained with hematoxylin and eosin. Samples of aorta and femoral artery were snap-frozen and embedded in optical coherence tomography Tissue Tek compound (Sakura, Chicago, Ill). Cryostat sections were blocked with 5% normal donkey serum (Jackson ImmunoResearch, Soham, UK) and stained with a polyclonal antibody raised against 2 smoothelin-specific peptides (described below) and a secondary antibody donkey–anti-rabbit conjugated with FITC (Sigma-Aldrich, St Louis, Mo).

Polyclonal antibody generation was performed by Eurogentec (Seraing, Belgium). Two rabbits were immunized with the smoothelin-B–specific peptide KRFRAERQDNKENWL (smoothelin-B residues 52 to 66) and the peptide RQRKRDQRDKERERR, which is present in both smoothelin-A and smoothelin-B (smoothelin-A residues 160 to 174, smoothelin-B residues 614 to 628). Synthesized peptides (5 mg) were conjugated to keyhole limpet hemocyanin. The rabbits received 3 booster injections with a 14-day interval. Sera were tested on different tissues for cross-reactivity and smooth muscle specificity.

To determine the staining pattern of the extracellular matrix proteins collagen and elastin, paraffin-embedded cross sections of arteries were stained with Sirius Red and Lawson's solution. To evaluate α-SMA and SM-MHC expression, sections were incubated with anti–α-SMA (DAKO, Glostrup, Denmark) or anti–SM-MHC antibody (Biomedical Technologies, Stoughton, Mass) diluted 1:200 or 1:40, respectively.

Vascular Contractility

Contractility of the thoracic aorta (n=10), saphenous artery (n=4), and femoral artery (n=6) was compared between 10-week-old *Smtn-B*$^{-/-}$ and *Smtn-B*$^{+/+}$ littermates. For the contractility analyses of *Smtn-A/B*$^{-/-}$ and *Smtn-A/B*$^{+/+}$ littermates, mice ≈8 weeks of age were used (n=7 for thoracic aorta and femoral artery). Isolated arteries were mounted in myograph organ baths as previously described.[18] We examined reactivity in response to K^+ (40 mmol/L), the thromboxane A_2 mimetic U-46619 (0.1 to 100 nmol/L), and the α_1-adrenergic agonist phenylephrine (0.1 to 30 μmol/L), all obtained from Sigma-Aldrich. Contractile forces were corrected for vessel segment length and medial thickness and normalized to wild-type values.

Hemodynamics

Five-month-old male *Smtn-B*$^{+/+}$ (n=7) and *Smtn-B*$^{-/-}$ (n=10) mice were instrumented with catheters as described before,[19] and conscious MAP and heart rate (HR) were recorded for 30 to 60 minutes on days 3 and 5 after surgery. In addition, the contribution of several endogenous neurohumoral mechanisms to blood pressure was assessed by the following pharmacological protocol. On day 3, MAP and HR responses were recorded during intravenous injection of phenylephrine (dose-response curve, 0.1 to 10 μg/kg in the presence of atropine [1.2 mg/kg] to block baroreflex-mediated bradycardia) and after administration of the β-blocker metoprolol (2.5 mg/kg). On day 5, MAP and HR responses to the α_1 blocker prazosin (0.1 mg/kg) and the α_2 blocker yohimbine (1 mg/kg) were recorded.

Pulse-wave velocity and pulse pressure were measured under isoflurane anesthesia by a high-fidelity catheter-tip micromanometer (Mikro-tip 1.4 F SPR-671, Millar Instruments, Houston, Tex) that was inserted via the left carotid artery into the aorta of *Smtn-B*$^{+/+}$ (n=7) and *Smtn-B*$^{-/-}$ (n=5) mice.

Because of their physical condition and short lifespan, hemodynamic parameters of *Smtn-A/B*$^{-/-}$ and *Smtn-A/B*$^{+/+}$ mice were measured in 6-week-old females under 1% to 2% isoflurane anesthesia via a catheter introduced into the right carotid artery (n=5 for each genotype).

Magnetic Resonance Imaging

Magnetic resonance imaging measurements were performed in eleven 8-month-old male mice of each genotype with a 6.3-T horizontal-bore animal scanner (Bruker BioSpin, Ettlingen, Germany) and a 3-cm-diameter birdcage radiofrequency coil (Rapid Biomedical, Rimpar, Germany). End-diastolic volume, end-systolic volume, stroke volume, ejection fraction, and left ventricular mass (1.05 g/cm^3)[20] were calculated from a semiautomatic segmentation of the images with the FARM MRV CAAS software provided by Pie Medical Imaging (Maastricht, the Netherlands).[21]

To determine the distension of the descending thoracic aorta during the cardiac cycle, a modified fast low-angle shot sequence was used with an in-plane navigator echo.[21] The distension of the thoracic aorta was measured manually at a fixed position for 7 *Smtn-B*$^{+/+}$ and 5 *Smtn-B*$^{-/-}$ mice. From these data, the relative distension as function of time and the maximum distension were derived.

Statistical Analysis

Statistical significance was calculated by 2-tailed Student *t* tests or repeated-measures 2-way ANOVA as indicated with Graphpad Prism software (version 4.0) and SPSS software (version 15.0; SPSS Inc, Chicago, Ill). Results were considered significantly different at values of $P<0.05$. Values are expressed as mean±SEM. The online-only Data Supplement provides a more detailed Methods section.

The authors had full access to and take full responsibility for the integrity of the data. All authors have read and agree to the manuscript as written.

Results

Smtn-B$^{-/-}$ Mice Develop Normally, Expressing Smoothelin-A but No Intact Smoothelin-B

To generate *Smtn-B*$^{-/-}$ mice, we replaced *Smtn* exons 3 through 7 with a neomycin-resistance cassette (Figure 1A and 1B). This deletion disrupts the smoothelin-B gene while leaving the smoothelin-A promoter intact.[22] Intercrosses of *Smtn-B*$^{+/-}$ mice produced *Smtn-B*$^{-/-}$ offspring at mendelian frequency (*Smtn-B*$^{+/+}$, 28%; *Smtn-B*$^{+/-}$, 50%; *Smtn-B*$^{-/-}$, 22%; n=506), indicating that loss of smoothelin-B does not interfere with embryonic survival. In contrast to *Smtn-A/B*$^{-/-}$ mice, which die rapidly after birth,[17] *Smtn-B*$^{-/-}$ mice appeared normal, had no gross histological abnormalities in any organ as evaluated by an experienced animal pathologist, and had unaltered intestinal function.[17]

Q-PCR analyses showed an absence of intact smoothelin-B transcripts in the aorta, femoral artery, and jejunum of *Smtn-B*$^{-/-}$ mice (Figure 1C). On the other hand, upregulation of either smoothelin-A or an interrupted smoothelin-B transcript still containing its 3′ smoothelin-A sequence was found in *Smtn-B*$^{-/-}$ blood vessels (Figure 1C). However, smoothelins were not detectable in the aorta of *Smtn-B*$^{-/-}$ mice by immunohistological stainings with polyclonal antibodies recognizing both smoothelin-A and smoothelin-B (Figure 1D). Thus, *Smtn-B*$^{-/-}$ mice display a null mutation in vascular tissue and can be used to delineate the role of smoothelin-B in vascular smooth muscle function. As predicted, *Smtn-B*$^{-/-}$ mice displayed normal smoothelin expression in visceral tissues (Figure 1C).

Normal Contractile Gene Expression and Normal Arterial Structure in *Smtn-B*$^{-/-}$ Mice

To study whether levels of important contractile smooth muscle–specific genes were altered by the loss of smoothelin-B, we examined the expression of α-SMA, SM-MHC, and SM-calponin in arteries of 6-month-old mice by

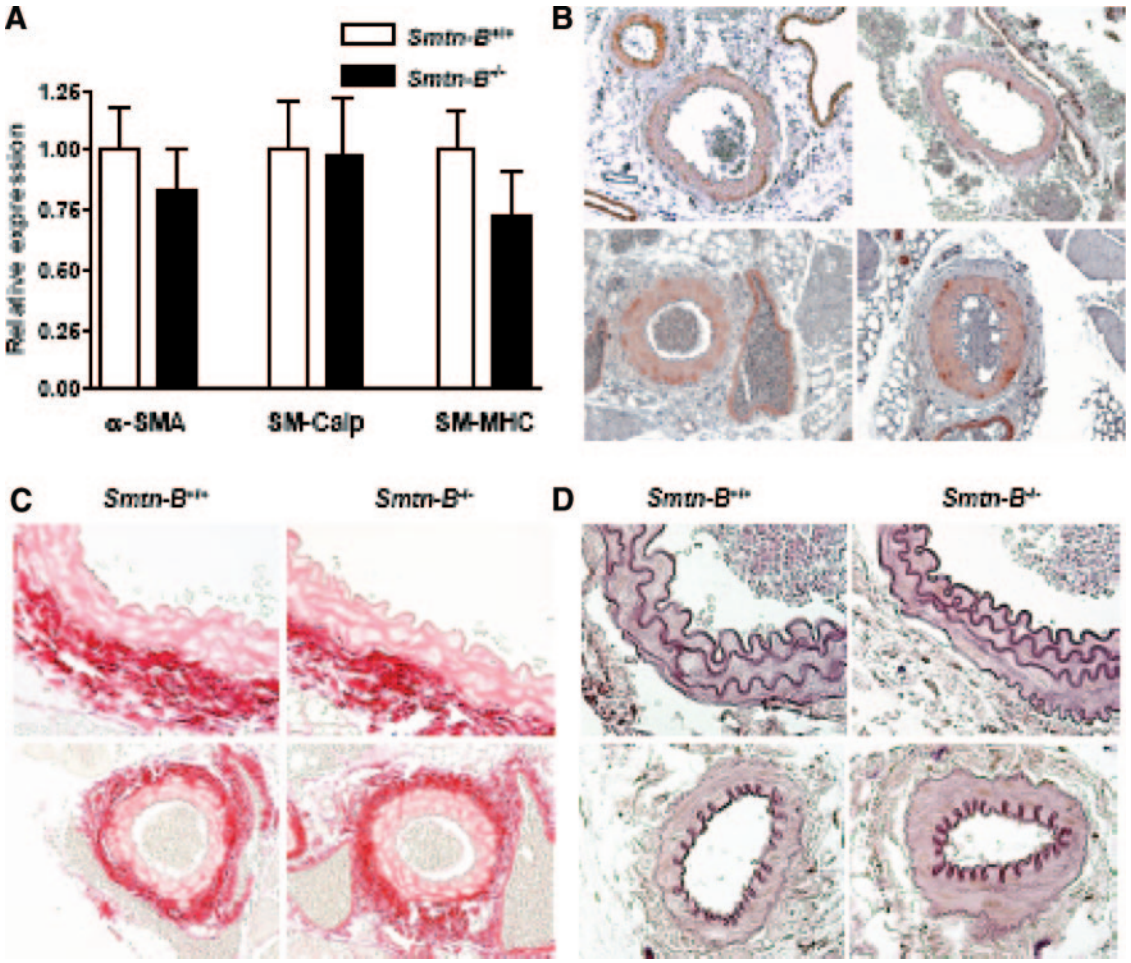

Figure 2. Normal contractile gene expression and arterial structure in *Smtn-B*$^{-/-}$ mice. A, Expression of α-SMA, SM-MHC, and SM-calponin (SM-Calp) was measured by Q-PCR (n=6 for each genotype). Levels were normalized to cyclophilin A expression, and *Smtn-B*$^{+/+}$ levels were set at 1. No significant change in expression levels was found between *Smtn-B*$^{+/+}$ and *Smtn-B*$^{-/-}$ mice. B, Representative immunohistochemical staining of α-SMA in the aorta (top; ×100 magnification) and femoral artery (bottom; ×200 magnification) of *Smtn-B*$^{-/-}$ and *Smtn-B*$^{+/+}$ mice showing no differences between the genotypes. C, Representative images of Sirius Red staining of the aorta (top; ×400 magnification) and femoral artery (bottom; ×200 magnification) of *Smtn-B*$^{-/-}$ and *Smtn-B*$^{+/+}$ mice showing no major differences in collagen content or distribution. D, Representative images of Lawson's elastin staining of the aorta (top; ×400 magnification) and femoral artery (bottom; ×200 magnification) of *Smtn-B*$^{-/-}$ and *Smtn-B*$^{+/+}$ mice showing regular elastic fibers in both genotypes.

Q-PCR (n=6 for each genotype). The expression of these components of the SMC contractile machinery was not significantly changed at the mRNA level (Figure 2A). In addition, both α-SMA (Figure 2B) and SM-MHC proteins (S.S.R., unpublished data, 2007) were readily detectable in medial SMCs of *Smtn-B*$^{-/-}$ mice. Moreover, the femoral artery and aorta of *Smtn-B*$^{-/-}$ mice appeared histologically normal and had a similar medial cross-sectional area and vessel radius compared with *Smtn-B*$^{+/+}$ mice (cross-sectional area of aorta, 0.086±0.004 versus 0.075±0.004 mm^2; cross-sectional area of femoral artery, 0.0107±0.0005 versus 0.0101±0.0005 mm^2; radius of aorta, 367±4 versus 349±10 μm; radius of femoral artery, 145±5 versus 143±5 μm for *Smtn-B*$^{+/+}$ versus *Smtn-B*$^{-/-}$ mice, respectively). The staining patterns of the extracellular matrix proteins collagen and elastin also were normal in *Smtn-B*$^{-/-}$ mice, showing regular arrangement of elastic fibers and laminae without fragmentation (Figure 2C and 2D). Hence, loss of smoothelin-B does not affect blood vessel architecture or the expression of other major smooth muscle contractile proteins.

Severely Compromised Arterial Contractile Capacity in *Smtn-B*$^{-/-}$ Mice

To examine the effect of smoothelin-B deficiency on vascular smooth muscle function, we measured contractility of the femoral artery and the saphenous artery, which contain high amounts of smoothelin-B. We also determined contractility of the thoracic aorta, which contains little smoothelin-B.[7] Several contractile agonists were applied to isolated vessel segments in a myograph to assess the integrity of different signal transduction pathways that activate SMC contraction. Because sensitivities to the contractile stimuli did not differ significantly between genotypes, only differences between maximal responses are discussed. Maximal contractile responses generated by aortas of *Smtn-B*$^{-/-}$ mice were attenuated during stimulation with K^+, the thromboxane A_2 mimetic U46619, or the α_1-adrenergic agonist phenylephrine, although the difference with *Smtn-B*$^{+/+}$ aortas was not significant (Figure 3A). In contrast, maximal contractions produced by both femoral and saphenous arteries of *Smtn-B*$^{-/-}$ mice were strongly and significantly decreased compared with

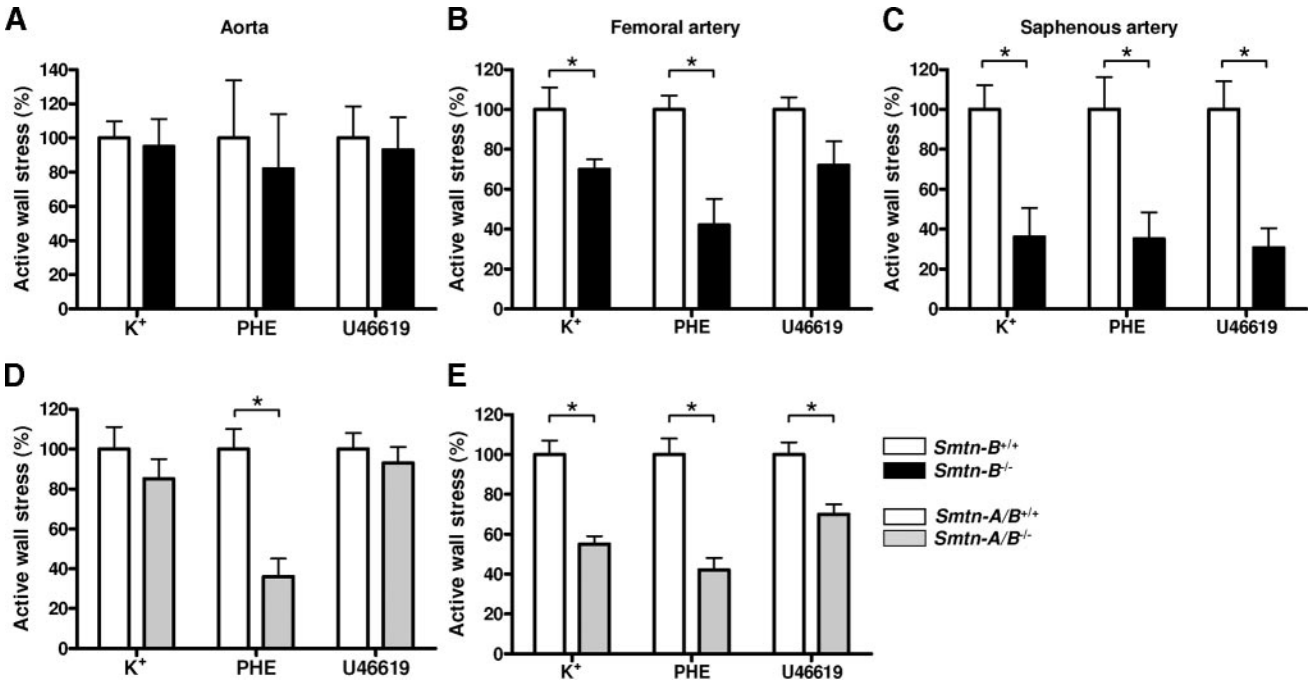

Figure 3. Decreased vascular smooth muscle contractility in *Smtn-B*$^{-/-}$ and *Smtn-A/B*$^{-/-}$ mice. Maximal contractile responses to K^+, phenylephrine (PHE), and U46619 of aorta (A; n=10 for each genotype), femoral artery (B; n=6 for each genotype), and saphenous artery (C; n=4 for each genotype) of *Smtn-B*$^{-/-}$ mice were diminished (femoral artery: K^+, $P=0.03$; PHE, $P<0.01$; saphenous artery: K^+, $P<0.01$; PHE, $P<0.01$; U46619, $P<0.01$). Maximal contractility of the aorta (D; n=7 for each genotype) and the femoral artery (E; n=7 for each genotype) of *Smtn-A/B*$^{-/-}$ mice was reduced to the same extent as in *Smtn-B*$^{-/-}$ mice (aorta: PHE, $P<0.01$; femoral artery: K^+, $P<0.05$; PHE, $P<0.01$; U46619, $P<0.05$). Active wall stress was normalized to wild-type values. *Statistically significant differences.

control mice (Figure 3B and 3C). Contractility of the femoral artery in response to phenylephrine was reduced by >50%. Maximal contractile responses of the saphenous artery to all 3 stimuli were reduced by 60% to 70%.

To investigate whether lack of smoothelin-A on top of smoothelin-B deficiency has an additional effect on vascular smooth muscle performance, we tested the same vasoactive compounds on arterial vessels isolated from *Smtn-A/B*$^{-/-}$ mice. Of note, *Smtn-A/B*$^{-/-}$ mice had a decreased medial cross-sectional area of the thoracic aorta and femoral artery that was proportional to their smaller body size.[17] The reduced smooth muscle volume was corrected for in the contractility analyses. Thoracic aortas of *Smtn-A/B*$^{-/-}$ mice displayed a more pronounced reduction of maximal responses to phenylephrine (Figure 3D). Femoral arteries of *Smtn-A/B*$^{-/-}$ mice showed greatly reduced contractility regardless of the type of agonist used to trigger contraction (Figure 3E). In general, the extent of the reductions were comparable to those observed in *Smtn-B*$^{-/-}$ vessels. Taken together, these data show that smoothelin-B is an important determinant of muscular artery contractility.

Increased MAP and Cardiac Hypertrophy in *Smtn-B*$^{-/-}$ Mice

The physiological consequences of the reduced arterial contractility in *Smtn-B*$^{-/-}$ mice were analyzed by measuring several hemodynamic parameters in conscious mice. Surprisingly, basal MAP was significantly higher in *Smtn-B*$^{-/-}$ mice than in control mice (≈20 mm Hg; $P<0.01$), whereas HR was not different (Figure 4A).

In line with the elevated MAP, *Smtn-B*$^{-/-}$ mice developed a significantly higher ratio of heart weight to body weight at 8

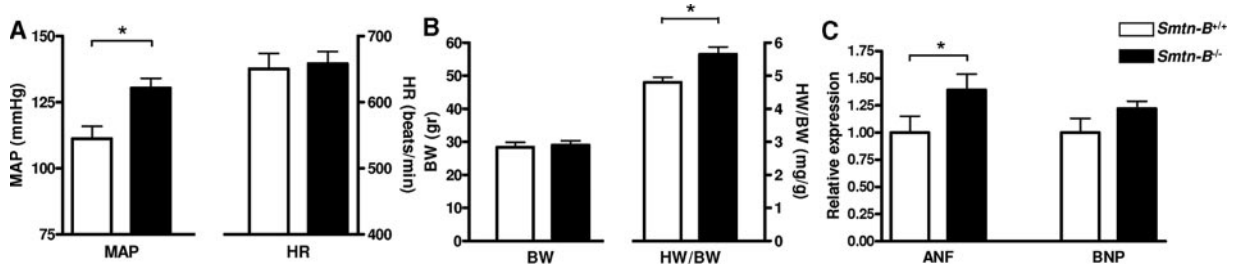

Figure 4. *Smtn-B*$^{-/-}$ mice develop elevated blood pressure and cardiac hypertrophy. A, *Smtn-B*$^{-/-}$ mice (n=10) displayed elevated MAP compared with *Smtn-B*$^{+/+}$ mice (n=7) ($P<0.01$), whereas HR was comparable. B, Ratio of heart weight to body weight (HW/BW) was increased ($P<0.01$), whereas BW was unaltered in *Smtn-B*$^{-/-}$ mice (*Smtn-B*$^{-/-}$, n=15; *Smtn-B*$^{+/+}$, n=13). C, Ventricular atrial natriuretic factor (ANF) and brain natriuretic peptide (BNP) levels as measured by Q-PCR were elevated in *Smtn-B*$^{-/-}$ mice ($P<0.05$, $P=0.08$, respectively; n=11 for each genotype). *Smtn-B*$^{+/+}$ levels were set at 1. *Statistically significant differences.

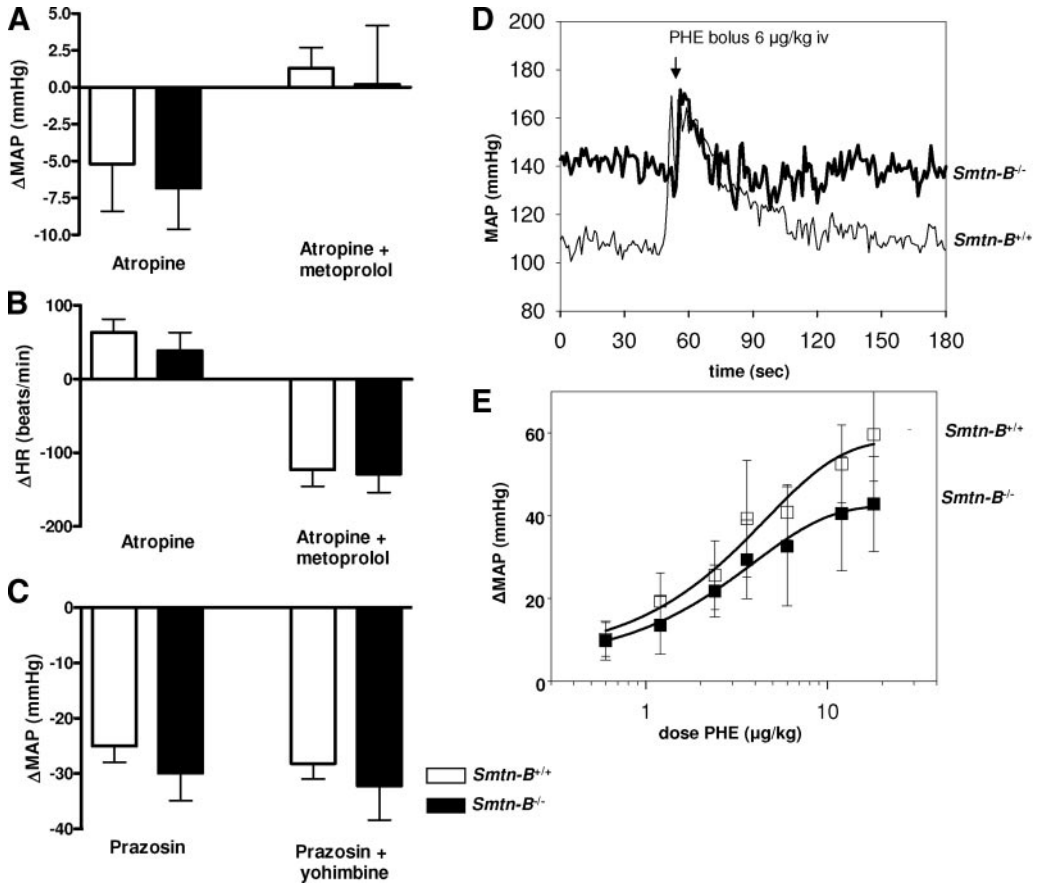

Figure 5. Normal blood pressure control in *Smtn-B*$^{-/-}$ mice. Changes in MAP (A) and HR (B) after muscarinic blockade by bolus injection of atropine followed by β_1 blockade using metoprolol were not different between *Smtn-B*$^{+/+}$ (n=7) and *Smtn-B*$^{-/-}$ mice (n=10). C, Full blockade of α_1-adrenergic receptors using prazosin or α_2-adrenergic receptors using yohimbine caused a similar decline in MAP in *Smtn-B*$^{+/+}$ (n=7) and *Smtn-B*$^{-/-}$ (n=10) mice. D, Representative tracings of pressor responses to an intravenous bolus of the α_1-agonist phenylephrine (PHE) in conscious unrestrained *Smtn-B*$^{+/+}$ (thin line) and *Smtn-B*$^{-/-}$ (thick line) mice. E, Comparison of the average pressor responses to a dose range of PHE in *Smtn-B*$^{+/+}$ (□; n=7) and *Smtn-B*$^{-/-}$ (■; n=10) mice. Data were compared by 2-way (genotype, dose) repeated-measures ANOVA.

months of age (Figure 4B). Morphometric analysis of the hearts of these mice showed that both the left and right ventricular walls were enlarged (left ventricle cross-sectional area, 13.4±0.1 versus 12.9±0.1 mm^2; right ventricle cross-sectional area, 5.4±0.6 versus 4.8±0.4 mm^2 for *Smtn-B*$^{-/-}$ versus *Smtn-B*$^{+/+}$ mice). The number of cardiomyocyte nuclei per 1 mm^2 was similar (79.8±3.0 versus 79.4±4.1 for *Smtn-B*$^{-/-}$ versus *Smtn-B*$^{+/+}$ littermates), consistent with a hypertrophic response. To establish whether the increased ratio of heart weight to body weight indeed reflected cardiac hypertrophy, we measured the expression of the cardiac hypertrophy markers atrial natriuretic factor and brain natriuretic peptide in the hearts of 8-month-old mice (n=11 for each genotype). mRNA levels of both natriuretic peptides were elevated in *Smtn-B*$^{-/-}$ mice compared with *Smtn-B*$^{+/+}$ littermates (Figure 4C).

Increased MAP and higher ratios of heart weight to body weight also were detected in *Smtn-A/B*$^{-/-}$ mice at the young age of only 6 weeks (MAP: 95±5 versus 87±2 mm Hg, $P<0.01$; ratio of heart weight to body weight: 6.8±0.9 versus 5.8±0.4 mg/g, $P<0.01$ for *Smtn-A/B*$^{-/-}$ versus *Smtn-A/B*$^{+/+}$ littermates). Collectively, these results show that smoothelin deficiency results in elevated blood pressure, leading to cardiac hypertrophy.

Normal Blood Pressure Control in *Smtn-B*$^{-/-}$ Mice

To determine whether the increased MAP in *Smtn-B*$^{-/-}$ mice was due to alterations in endogenous blood pressure control mechanisms, we determined MAP and HR after injection of several autonomic nervous system blockers in conscious mice. *Smtn-B*$^{-/-}$ and *Smtn-B*$^{+/+}$ mice displayed similar changes in MAP and HR after administration of atropine or atropine plus metoprolol (Figure 5A and 5B), indicating that cardiac parasympathetic tone and sympathetic tone were comparable. In addition, the MAP response to the α-adrenergic blockers prazosin and yohimbine did not differ between *Smtn-B*$^{+/+}$ and *Smtn-B*$^{-/-}$ mice (Figure 5C). Thus, no difference exists in autonomic control that may explain the different MAP between the genotypes. In line with the myograph data, MAP responses to intravenous bolus injections of the α_1-adrenergic agonist phenylephrine were lower in *Smtn-B*$^{-/-}$ mice than in *Smtn-B*$^{+/+}$ mice, although the differences were not significantly different at any dose (Figure 5D and 5E).

Normal Cardiac Function but Increased Peripheral Vascular Resistance in *Smtn-B*$^{-/-}$ Mice

The distensibility of the large arteries affects central arterial pressure. Therefore, we first investigated whether decreased distensibility in *Smtn-B*$^{-/-}$ animals contributes to the elevated

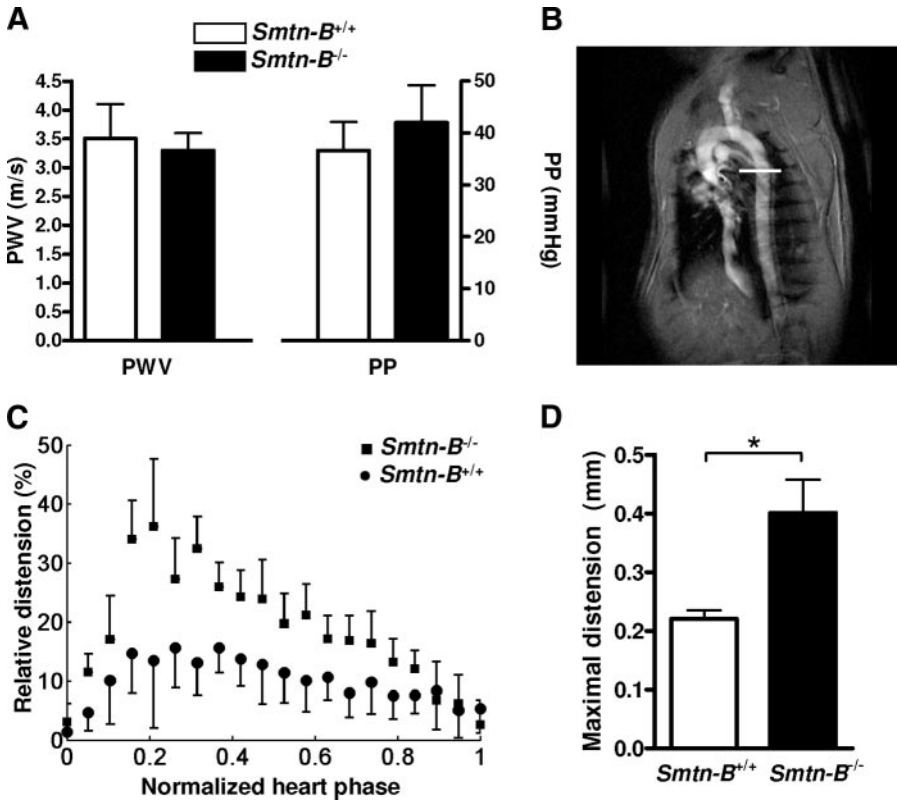

Figure 6. Increased aortic distension but normal aortic distensibility in *Smtn-B*$^{-/-}$ mice. A, Pulse-wave velocity (PWV) and pulse pressure (PP) measurements at comparable HRs and MAPs show no difference between *Smtn-B*$^{-/-}$ (n=5) and *Smtn-B*$^{+/+}$ (n=7) mice, indicating normal aortic distensibility. B, MR image of the aorta of a *Smtn-B*$^{+/+}$ mouse at the end-diastolic heart phase. The white line indicates the position of the lumen diameter measurement. C, Aortic distension in *Smtn-B*$^{-/-}$ mice (■) was increased throughout the cardiac cycle compared with *Smtn-B*$^{+/+}$ mice (●). The beginning of the systolic heart phase is represented by 0, the end-diastolic phase by 1. D, Maximal distension was almost 2-fold greater in *Smtn-B*$^{-/-}$ mice (*Smtn-B*$^{-/-}$, n=5; *Smtn-B*$^{+/+}$, n=7). *Statistically significant differences.

MAP. We measured pulse-wave velocity and pulse pressure in the thoracic aorta. At comparable HRs (573±36 versus 562±38 bpm for *Smtn-B*$^{-/-}$ and *Smtn-B*$^{+/+}$ animals; $P=0.80$) and comparable MAPs (89±9 versus 86±1 mm Hg for *Smtn-B*$^{-/-}$ and *Smtn-B*$^{+/+}$ animals; $P=0.45$), no significant difference was found in either pulse-wave velocity or pulse pressure (Figure 6A), demonstrating unchanged aortic distensibility in *Smtn-B*$^{-/-}$ mice.

MAP is by definition the product of cardiac output and total peripheral vascular resistance. Consequently, the elevated MAP in *Smtn-B*$^{-/-}$ mice might arise from increases in either or both of these factors. We first analyzed cardiac output by magnetic resonance imaging. Stroke volume, HR, and cardiac output did not differ between *Smtn-B*$^{-/-}$ and *Smtn-B*$^{+/+}$ littermates (Table). Because cardiac output was not increased, the elevated MAP in *Smtn-B*$^{-/-}$ mice had to be due to increased peripheral vascular resistance. Analysis of the distension of the aorta during the cardiac cycle by magnetic resonance imaging (Figure 6B) revealed increased distension in *Smtn-B*$^{-/-}$ mice throughout the cardiac cycle (Figure 6C). The maximal distension was almost 2-fold greater for *Smtn-B*$^{-/-}$ mice ($P=0.01$; Figure 6D). The lumen diameter of the thoracic aorta at the end-diastolic heart phase was 1.15±0.15 versus 1.05±0.17 mm for the *Smtn-B*$^{-/-}$ and *Smtn-B*$^{+/+}$ mice, respectively. The increased aortic distension despite similar aortic distensibility and comparable cardiac output implies the presence of increased peripheral vascular resistance, which causes elevated MAP in *Smtn-B*$^{-/-}$ mice.

Table. Characteristics of Cardiac Function of *Smtn-B*$^{-/-}$ (n=11) and *Smtn-B*$^{+/+}$ (n=11) Mice as Measured by Magnetic Resonance Imaging

Parameter	*Smtn-B*$^{-/-}$	*Smtn-B*$^{+/+}$
End-diastolic volume, μL	44±2.6	47±2.1
End-systolic volume, μL	10±0.8	13±1.2
Ejection fraction, %	76±1.1	73±1.2*
Left ventricular mass, mg	114±2.7	101±4.5*
Stroke volume, μL	34±2.0	34±1.1
HR, bpm	521±11	527±6
Cardiac output, mL/min	17.7±1.0	18.1±0.7

*$P=0.02$.

Discussion

The present study was instigated by our recent demonstration that mice lacking both smoothelin isoforms display markedly reduced intestinal smooth muscle contraction.[17] In line with this, we show here that loss of the vascular-specific smoothelin-B protein leads to greatly diminished vascular contractile capacity. Paradoxically, this is accompanied by elevated MAP and cardiac hypertrophy. Because cardiac output, autonomic nervous system activity, and large-artery properties are not altered in smoothelin-B–deficient mice, the increased pressure must have its origin in altered microvascular properties. The data obtained in this study provide the first evidence that smoothelin-B is essential for vascular smooth muscle performance.

Reduced contractility of *Smtn-B*$^{-/-}$ muscular arteries was observed regardless of the signal transduction pathways activated. Together with the binding of smoothelin-B to the contractile filaments,[23] this nonselective reduction of contractility suggests that smoothelin-B plays a role at the core of the

vascular SMC contractile machinery. The mechanism by which smoothelin-B affects smooth muscle contraction needs more study. The cardiovascular phenotype of other knockout mouse models of contractile SMC proteins has been shown to be due to downregulation of other proteins involved in SMC contraction, upregulation of related proteins, or expression of different alternatively spliced contractile proteins.[2,3,24,25] We have excluded the possibility that downregulation of the most important SMC contractile genes is responsible for the phenotype of *Smtn-B*$^{-/-}$ mice. In addition, smoothelin homologs are not detected by database searches, making it unlikely that upregulation of such proteins can compensate for the loss of smoothelin function. It cannot be completely ruled out, however, that changes in alternative splicing or organization of other contractile proteins occur in *Smtn-B*$^{-/-}$ animals.

An important determinant of the amount of contractile force in muscle contraction is the degree of cooperativity between multiple actomyosin cross-bridges. Cooperativity in skeletal muscle is coordinated by tropomyosin and the troponin proteins.[26] However, troponins are not expressed in SMCs. Instead, smooth muscle tropomyosin interacts with h-caldesmon and SM-calponin, which partly take over the role of troponins.[5] Importantly, smoothelins contain a 37–amino acid sequence that is similar to the tail domain of troponin T.[10] In skeletal muscle, this domain not only is required for troponin T interaction with tropomyosin but also is involved in the activation of actomyosin ATPase.[27] Thus, smoothelins might be part of a smooth muscle tropomyosin-troponin–like system. The diminished contractile potential of vascular smooth muscle of *Smtn-B*$^{-/-}$ mice may be due to a lack of cooperativity of contraction, which then would depend on a functional smoothelin-tropomyosin system.

Surprisingly, the reduced contractile capacity of smoothelin-B–deficient muscular arteries ex vivo was accompanied by elevated blood pressure in *Smtn-B*$^{-/-}$ mice. However, reduced maximal vascular contractility does not necessarily manifest itself in the MAP. Elevation of mean blood pressure may occur as a result of increased cardiac output, increased total peripheral resistance, or their combination. The magnetic resonance imaging measurements in this study show that cardiac output in the *Smtn-B*$^{-/-}$ mice is not changed. Therefore, the peripheral resistance of the vasculature must be affected by the mutation, which is conceivable considering the significant expression of smoothelin-B in the smaller vessels. The increased aortic distension despite similar cardiac output and similar aortic structure, diameter, and distensibility in *Smtn-B*$^{-/-}$ mice supports that increased resistance to blood flow is brought about by the smaller downstream parts of the vascular tree.

It is unlikely that the increased MAP is caused by overactivity of the autonomic nervous system because neither blockade of muscarinic receptors nor blockade of β_1- or $\alpha_{1/2}$-adrenergic receptors revealed differences in blood pressure response and because HR did not differ between the genotypes either. However, changes in other neurohumoral vasopressor systems that control blood pressure, changes in arterial relaxation properties, or differences in the total number of vessels might contribute to the altered MAP in *Smtn-B*$^{-/-}$ mice. In addition, we cannot rule out that smoothelin deficiency might have a stimulatory effect on arteriole contractility.

Overall, the cardiovascular phenotype of *Smtn-B*$^{-/-}$ mice is similar to that of patients with established hypertension. They, too, have a normal cardiac output with a hypertrophic heart, accompanied by increased peripheral resistance.[28]

Two other observations in this study deserve further comment. First, we found no indications of SMC phenotype changes such as decreased contractile gene expression or altered cell morphology in *Smtn-B*$^{-/-}$ mice. Therefore, it is unlikely that smoothelin-B plays a role in the regulation of SMC differentiation, as was previously suggested on the basis of its strict contractile phenotype-specific expression.[23] Second, arterial contractility was similarly reduced in mice lacking both smoothelins and mice lacking only smoothelin-B, indicating that smoothelin-B is the functional smoothelin isoform in vascular smooth muscle.

Conclusions

The data in this study show that smoothelin-B deficiency causes a major decline in the contractile performance of vascular smooth muscle. Instead of merely reflecting the SMC contractile phenotype, smoothelins appear to actively participate in the contractile process itself. Mutations in the *Smtn* gene or alterations in smoothelin levels may therefore contribute to the development of hypertension and concomitant cardiac hypertrophy in humans.

Acknowledgments

We would like to thank Agnieszka Strzelecka, Jacques Debets, Gregorio Fazzi, Darren Baker, and our colleagues from the animal facility for expert technical assistance in various aspects of the study.

Sources of Funding

This work was supported by grants from the Netherlands Heart Foundation (97.167), Stichting De Gelderfonds, Stichting Simonsfonds, and The Netherlands Organization for Scientific Research (Dr Rensen); the European Vascular Genomics Network and the EC-FP6-project DiMI, LSHB-CT-2005–512146 (Dr de Mey); and the BSIK program Molecular Imaging of Ischemic Heart Disease (BSIK03033) (E. Heijman and Dr Strijkers). Dr Niessen was supported by a Kootstra fellowship from Maastricht University.

Disclosures

None.

References

1. Cowley AW Jr. The genetic dissection of essential hypertension. *Nat Rev Genet*. 2006;7:829–840.
2. Schildmeyer LA, Braun R, Taffet G, Debiasi M, Burns AE, Bradley A, Schwartz RJ. Impaired vascular contractility and blood pressure homeostasis in the smooth muscle alpha-actin null mouse. *FASEB J*. 2000;14:2213–2220.
3. Babu GJ, Loukianov E, Loukianova T, Pyne GJ, Huke S, Osol G, Low RB, Paul RJ, Periasamy M. Loss of SM-B myosin affects muscle shortening velocity and maximal force development. *Nat Cell Biol*. 2001;3:1025–1029.
4. Masuki S, Takeoka M, Taniguchi S, Yokoyama M, Nose H. Impaired arterial pressure regulation during exercise due to enhanced muscular vasodilatation in calponin knockout mice. *J Physiol*. 2003;553:203–212.
5. Morgan KG, Gangopadhyay SS. Invited review: cross-bridge regulation by thin filament-associated proteins. *J Appl Physiol*. 2001;91:953–962.
6. van der Loop FT, Schaart G, Timmer ED, Ramaekers FC, van Eys GJ. Smoothelin, a novel cytoskeletal protein specific for smooth muscle cells. *J Cell Biol*. 1996;134:401–411.

7. van der Loop FT, Gabbiani G, Kohnen G, Ramaekers FC, van Eys GJ. Differentiation of smooth muscle cells in human blood vessels as defined by smoothelin, a novel marker for the contractile phenotype. *Arterioscler Thromb Vasc Biol*. 1997;17:665–671.
8. Johnson JL, van Eys GJ, Angelini GD, George SJ. Injury induces dedifferentiation of smooth muscle cells and increased matrix-degrading metalloproteinase activity in human saphenous vein. *Arterioscler Thromb Vasc Biol*. 2001;21:1146–1151.
9. Christen T, Verin V, Bochaton-Piallat M, Popowski Y, Ramaekers F, Debruyne P, Camenzind E, van Eys G, Gabbiani G. Mechanisms of neointima formation and remodeling in the porcine coronary artery. *Circulation*. 2001;103:882–888.
10. Quensel C, Kramer J, Cardoso MC, Leonhardt H. Smoothelin contains a novel actin cytoskeleton localization sequence with similarity to troponin T. *J Cell Biochem*. 2002;85:403–409.
11. Rensen S, Thijssen V, De Vries C, Doevendans P, Detera-Wadleigh S, Van Eys G. Expression of the smoothelin gene is mediated by alternative promoters. *Cardiovasc Res*. 2002;55:850–863.
12. Bar H, Wende P, Watson L, Denger S, van Eys G, Kreuzer J, Jahn L. Smoothelin is an indicator of reversible phenotype modulation of smooth muscle cells in balloon-injured rat carotid arteries. *Basic Res Cardiol*. 2002; 97:9–16.
13. Maeng M, Mertz H, Nielsen S, Van Eys GJ, Rasmussen K, Espersen GT. Adventitial myofibroblasts play no major role in neointima formation after angioplasty. *Scand Cardiovasc J*. 2003;37:34–42.
14. Verhamme P, Quarck R, Hao H, Knaapen M, Dymarkowski S, Bernar H, Van Cleemput J, Janssens S, Vermylen J, Gabbiani G, Kockx M, Holvoet P. Dietary cholesterol withdrawal reduces vascular inflammation and induces coronary plaque stabilization in miniature pigs. *Cardiovasc Res*. 2002;56:135–144.
15. Tharp DL, Wamhoff BR, Turk JR, Bowles DK. Upregulation of intermediate-conductance Ca^{2+}-activated K^+ channel (IKCa1) mediates phenotypic modulation of coronary smooth muscle. *Am J Physiol Heart Circ Physiol*. 2006;291:H2493–H2503.
16. Hao H, Gabbiani G, Camenzind E, Bacchetta M, Virmani R, Bochaton-Piallat ML. Phenotypic modulation of intima and media smooth muscle cells in fatal cases of coronary artery lesion. *Arterioscler Thromb Vasc Biol*. 2006;26:326–332.
17. Niessen P, Rensen S, van Deursen J, De Man J, De Laet A, Vanderwinden JM, Wedel T, Baker D, Doevendans P, Hofker M, Gijbels M, van Eys G. Smoothelin-a is essential for functional intestinal smooth muscle contractility in mice. *Gastroenterology*. 2005;129:1592–1601.
18. Raat NJ, Wetzels GE, De Mey JG. Calcium-contraction relationship in rat mesenteric arterial smooth muscle: effects of exogenous and neurogenic noradrenaline. *Pflugers Arch*. 1998;436:262–269.
19. Janssen BJ, Leenders PJ, Smits JF. Short-term and long-term blood pressure and heart rate variability in the mouse. *Am J Physiol Regul Integr Comp Physiol*. 2000;278:R215–R225.
20. Franco F, Dubois SK, Peshock RM, Shohet RV. Magnetic resonance imaging accurately estimates LV mass in a transgenic mouse model of cardiac hypertrophy. *Am J Physiol*. 1998;274:H679–H683.
21. Heijman E, de Graaf W, Niessen P, Nauerth A, van Eys G, de Graaf L, Nicolay K, Strijkers GJ. Comparison between prospective and retrospective triggering for mouse cardiac MRI. *NMR Biomed.* 2007;20:439–447.
22. Rensen SS, Niessen PM, Long X, Doevendans PA, Miano JM, van Eys GJ. Contribution of serum response factor and myocardin to transcriptional regulation of smoothelins. *Cardiovasc Res*. 2006;70:136–145.
23. Niessen P, Clement S, Fontao L, Chaponnier C, Teunissen B, Rensen S, van Eys G, Gabbiani G. Biochemical evidence for interaction between smoothelin and filamentous actin. *Exp Cell Res*. 2004;292:170–178.
24. Matthew JD, Khromov AS, McDuffie MJ, Somlyo AV, Somlyo AP, Taniguchi S, Takahashi K. Contractile properties and proteins of smooth muscles of a calponin knockout mouse. *J Physiol.* 2000;529(pt 3):811–824.
25. Morano I, Chai GX, Baltas LG, Lamounier-Zepter V, Lutsch G, Kott M, Haase H, Bader M. Smooth-muscle contraction without smooth-muscle myosin. *Nat Cell Biol*. 2000;2:371–375.
26. Marston SB, Redwood CS. The essential role of tropomyosin in cooperative regulation of smooth muscle thin filament activity by caldesmon. *J Biol Chem*. 1993;268:12317–12320.
27. Perry SV. Vertebrate tropomyosin: distribution, properties and function. *J Muscle Res Cell Motil*. 2001;22:5–49.
28. Mayet J, Hughes A. Cardiac and vascular pathophysiology in hypertension. *Heart*. 2003;89:1104–1109.

CLINICAL PERSPECTIVE

The causes of essential hypertension remain largely unknown, although it is commonly accepted that vascular smooth muscle dysfunction is a potential culprit. Improved insight into the mechanics and regulation of smooth muscle contraction may provide additional therapeutic targets to treat pathologies such as hypertension. However, our current understanding of these 2 aspects of smooth muscle function is limited. Here, we introduce smoothelin, a protein specifically expressed in fully differentiated, contractile smooth muscle cells, as a crucial component of the vascular smooth muscle cell contractile apparatus. We demonstrate for the first time that smoothelin is necessary for physiological vascular smooth muscle contraction. Smoothelin deficiency in mice resulted in severely reduced contractile potential, particularly in smaller arteries. Paradoxically, this was accompanied by hypertension and concomitant cardiac hypertrophy. Analyses of differently sized blood vessels indicated that the cause of the hypertension is likely to be downstream of vessels like the saphenous artery and/or mediated by overcompensation of blood pressure regulatory systems like the renin-angiotensin system. Recently, imatinib, a drug used in clinical practice, was shown to specifically promote smoothelin expression in vascular smooth muscle cells. Considering the currently reported data, such an increase in smoothelin concentration not only may indicate a more contractile phenotype of the vascular smooth muscle cell but also may improve vascular smooth muscle contractile potential. The combination of an increased knowledge of smoothelin function and the availability of pharmacological tools that affect smoothelin expression provides interesting opportunities to treat pathologies originating from vascular smooth muscle cell dysfunction.